

Sofia Macedo · Edward P. Mitchell · Célia V. Romão  
Serena J. Cooper · Ricardo Coelho · Ming Y. Liu  
António V. Xavier · Jean LeGall · Susan Bailey  
C. David Garner · Wilfred R. Hagen · Miguel Teixeira  
Maria A. Carrondo · Peter Lindley

## Hybrid cluster proteins (HCPs) from *Desulfovibrio desulfuricans* ATCC 27774 and *Desulfovibrio vulgaris* (Hildenborough): X-ray structures at 1.25 Å resolution using synchrotron radiation

Received: 9 October 2001 / Accepted: 28 November 2001 / Published online: 23 January 2002  
© SBIC 2002

**Abstract** The structures of the hybrid cluster proteins (HCPs) from the sulfate-reducing bacteria *Desulfovibrio desulfuricans* (ATCC 27774) and *Desulfovibrio vulgaris* (Hildenborough) have been elucidated at a resolution of 1.25 Å using X-ray synchrotron radiation techniques. In the case of the *D. desulfuricans* protein, protein isolation, purification, crystallization and X-ray data collection were carried out under strict anaerobic conditions, whereas for the *D. vulgaris* protein the conditions were

aerobic. However, both structures are essentially the same, comprising three domains and two iron-sulfur centres. One of these centres situated near the exterior of the molecules in domain 1 is a cubane [4Fe-4S] cluster, whereas the other, located at the interface of the three domains, contains the unusual four-iron cluster initially found in the *D. vulgaris* protein. Details of the structures and the associated EPR spectroscopy of the *D. desulfuricans* protein are reported herein. These structures show that the nature of the hybrid cluster, containing both oxygen and sulfur bridges, is independent of the presence of oxygen in the isolation and crystallization procedure and also does not vary significantly with changes in the oxidation state. The structures and amino acid sequences of the HCP are compared with the recently elucidated structure of the catalytic subunit of a carbon monoxide dehydrogenase from *Carboxythermus hydrogenoformans* and related dehydrogenases. Electronic supplementary material to this paper can be obtained by using the Springer Link server located at <http://dx.doi.org/10.1007/s00775-001-0326-y>.

Electronic supplementary material to this paper can be obtained by using the Springer Link server located at <http://dx.doi.org/10.1007/s00775-001-0326-y>.

S. Macedo · E.P. Mitchell · P. Lindley (✉)  
ESRF, BP-220, 38043 Grenoble Cedex, France  
E-mail: lindley@esrf.fr  
Tel.: +33-(0)4 76 88 20 14

S. Macedo · C.V. Romão · R. Coelho · A.V. Xavier  
M. Teixeira · M.A. Carrondo  
Instituto de Tecnologia Química e Biológica,  
Universidade Nova de Lisboa, Av. República,  
EAN, Apartado 127, 2781-901 Oeiras, Portugal

S.J. Cooper · S. Bailey  
CLRC Daresbury Laboratory, Daresbury,  
Warrington WA4 4AD, UK

S.J. Cooper · C.D. Garner  
School of Chemistry, University Park,  
Nottingham NG7 2RD, UK

M.Y. Liu · J. LeGall  
Department of Biochemistry, University of Georgia,  
Athens, GA 30602, USA

W.R. Hagen  
Delft University of Technology,  
Kluyver Department of Biotechnology,  
Julianalaan 67, 2628 BC Delft, The Netherlands

*Present address:* S. Bailey  
Lawrence Berkeley National Laboratory,  
1 Cyclotron Road, Mailstop 6-2132,  
Berkeley, CA 94720, USA

**Keywords** Hybrid cluster proteins · X-ray structure · Anaerobic *Desulfovibrio desulfuricans* · Aerobic *Desulfovibrio vulgaris*

### Introduction

Hybrid-cluster proteins (HCPs) were initially purified from two sulfate-reducing bacteria, *Desulfovibrio vulgaris* (Hildenborough) (*Dv*) and *Desulfovibrio desulfuricans* ATCC 27774 (*Dd*) [1, 2, 3]. The initial EPR spectroscopic analyses indicated that these HCPs had unprecedented redox chemistry and the presence of a [6Fe-6S] cluster was proposed [1, 2, 3, 4]. Thus, the protein was initially named the “prismane protein”. The first X-ray crystal structure of the aerobically purified *Dv* protein, at a resolution of 1.7 Å, showed that the HCP

does not contain a [6Fe-6S] cluster [5] but instead has two independent 4Fe centres. One of these is a canonical cubane [4Fe-4S]<sup>2+/1+</sup> type and the second is a novel cluster with a so-far unique arrangement containing two sulfur bridges, two oxo-iron bridges and an unknown ligand bridging two iron atoms. This new cluster was named the “hybrid cluster” and can be considered as comprising a 3Fe moiety and an iron atom bound to the protein by three protein ligands, a cysteine, a histidine and a glutamate. The 3Fe moiety contains a [2Fe-2S] group, with each iron linked to the protein by a cysteine residue and an iron atom bound to one of the inorganic sulfurs and linked to the protein by a glutamate and a persulfide group. This cluster is located at the interface of the three domains in the structure and is some 12 Å distant from the cubane cluster situated near the exterior of the protein in domain 1 [5, 6]. All the various spectroscopic studies have been re-analysed and found to be compatible with this structural model. Resonance Raman studies indicate that in the aerobic preparation of the *Dv* protein the unknown ligand is probably an oxygen atom (or OH<sup>-</sup> moiety). The hybrid centre has four oxidation states, ranging from the most oxidized state (+6) containing four Fe(III) atoms to the fully reduced state (+3) with three Fe(II) and one Fe(III) atoms. It behaves magnetically as a single entity resulting from the exchange coupling of the four high-spin Fe(III)/Fe(II) cations. Upon successive one-electron reduction and starting from the fully oxidized protein, four redox states are detected for the hybrid cluster. These states have system spins of  $S=0$ , 9/2 (and 1/2), 0 (and 4) and 1/2, respectively [2, 4, 7]. These redox properties, multiple redox states in a narrow and physiological potential range, are unique among metal centres in biological systems.

Despite the wealth of spectroscopic and structural information on HCPs, the precise physiological function(s) of these proteins remains unknown. HCPs are present in several anaerobic and facultative bacteria, as well as in anaerobic archaea. In *Escherichia coli* and *Morganella morganii* it was shown that HCP is expressed under mainly anaerobic conditions. Since this induction was seen in the presence of either nitrate or nitrite, it was proposed that the protein may be involved in anaerobic nitrate/nitrite respiration [8]. However, to date, no enzymatic activity for HCP has been clearly defined.

The quite unusual and unexpected structure of the hybrid cluster raised the question of whether it was indeed a native structure, or a result of some oxidative degradation upon isolation and purification of the protein in the presence of oxygen. In order to confirm this unique structure, it was essential to study other homologous proteins. Hence, the similar protein from *Dd*, a sulfate-reducing bacterium that also has the capability of using nitrate as a terminal electron acceptor, was crystallized. To avoid any possible oxidative damages the protein was purified and crystallized anaerobically. X-ray data for the *Dd* protein were initially collected at

a wavelength of 1.722 Å, so that anomalous dispersion effects could be used to confirm the locations of the iron atoms in the clusters. A second high-resolution data set, at 1.25 Å, was then collected using a wavelength of 0.933 Å. In addition, the resolution of the structure of the *Dv* protein was extended to 1.25 Å in an attempt to give a better definition for the hybrid cluster. The resultant crystallographic and spectroscopic studies are reported herein.

## Materials and methods

### Purification of the *Dd* protein

Anaerobic wild-type HCP was purified from the sulfate-reducing bacterium *Dd*, grown on a lactate/nitrate medium as previously described [9]. The cell-free extract was prepared under argon to avoid exposure to air, as described by LeGall et al. [10]. All purification procedures were performed at 4 °C and pH 7.6 in a Coy anaerobic chamber, model A-2463, under an argon/hydrogen atmosphere with  $p_{O_2} < 1$  ppm. Concentrations were performed in a Diaflo apparatus (Amicon, Danvers, Mass., USA) with a YM3 membrane.

The anaerobically prepared soluble extract (800 mL) was loaded on to a DEAE-52 column (6×34 cm; 1 mL/min), previously equilibrated with 10 mM Tris-HCl and a two-step (2 L each) Tris-HCl linear gradient (10–250 mM and 250–400 mM, respectively) was applied. The fraction containing HCP eluted at ~200 mM. Further purification included a passage on a DEAE Biogel column (5×41 cm; 0.5 mL/min), eluted in a continuous gradient (1 L) of 10–450 mM Tris-HCl. The HCP-rich fraction eluted at 300 mM, and was next applied to a hydroxyapatite column (3×20 cm; 0.6 mL/min) previously equilibrated with 200 mM Tris-HCl. Elution using a 0.4 L descending linear gradient (200–10 mM) of Tris-HCl was followed by a 1 L ascending linear gradient of 10–600 mM potassium phosphate buffer. The HCP-containing fraction eluted at 300 mM. The last step of purification was carried out on a Superdex 75 (XK 16/60) column using 20 mM Tris-HCl and 0.2 M NaCl (0.5 mL/min) as elution buffer. The purity achieved was verified with a 15% SDS-PAGE gel and UV-visible spectra.

### EPR spectroscopy

EPR spectra were recorded on a Bruker ESP 300 spectrometer, equipped with an Oxford Instruments helium flow cryostat. Samples for EPR spectroscopy were prepared inside the anaerobic chamber after letting the EPR tubes fully exchange with the chamber atmosphere. After filling the tubes with the samples (300 mL), they were sealed with Suba seal caps and frozen in liquid nitrogen immediately after being removed from the chamber. The samples were reduced with a freshly prepared sodium dithionite solution in 500 mM Tris-HCl buffer at pH 9.0.

### Crystallization

#### *The HCP from Dd*

Crystals of HCP isolated from *Dd* were grown in a nitrogen environment inside a glove box system ( $p_{O_2} < 1$  ppm) at 293 K by the sitting drop vapour-diffusion method. The best crystals were obtained using 25% PEG 4000 as precipitating agent and 0.1 M MES as buffer, at pH 6.0. Protein solution, 1.5 µL, (12.6 mg/mL in 20 mM Tris-HCl, pH 7.6, and 0.2 M NaCl) and an equal amount of precipitant solution were allowed to equilibrate against 500 µL of the latter in the reservoir. Needle-type pale yellow crystals required a long time to grow (4 months or longer) to a maximum size of approximately 0.02 mm×0.08 mm×0.16 mm.

**Table 1** Data collection statistics

	<i>D. desulfuricans</i>	<i>D. desulfuricans</i>	<i>D. vulgaris</i>
Beamline	BM14: ESRF	ID14-2: ESRF	9.6: SRS Daresbury
Space group	<i>P1</i>	<i>P1</i>	<i>P2<sub>1</sub>2<sub>1</sub>2<sub>1</sub></i>
Resolution (Å)	2.6	1.25	1.25
Highest res. shell (Å)	2.69–2.60	1.29–1.25	1.34–1.25
Wavelength (Å)	1.722	0.933	0.87
Cell dimensions			
<i>a</i> (Å)	57.4	57.33	63.81
<i>b</i> (Å)	61.8	61.65	64.53
<i>c</i> (Å)	72.2	72.25	151.87
$\alpha$ (°)	82.7	82.77	90
$\beta$ (°)	73.7	73.67	90
$\gamma$ (°)	87.3	87.31	90
Total no. of <i>hkl</i>	114,637	915,955	400,513
No. of batches and rotation angle (°)	450/1.0	360/1.0	299/0.5
Number of unique <i>hkl</i>	27,761	247,243	163,543
Average multiplicity	4.1 (4.1)	3.7 (3.7)	2.4 (1.7)
$R_{\text{merge}}^a$	0.08 (0.13)	0.054 (0.215)	0.063 (0.331)
Average $I/\sigma(I)$	4.2 (2.6)	8.0 (3.1)	6.2 (1.6)
Completeness (%)	95.9 (94.5)	94.9 (85.3)	94.6 (86.4)
Completeness for anomalous data (%)	92.2 (91.1)	–	–
Average <i>B</i> (Wilson) (Å <sup>2</sup> )	27.8	7.2	10.9

<sup>a</sup> $R_{\text{merge}}$  is  $\Sigma|I - \langle I \rangle| / \Sigma \langle I \rangle$

### The HCP from *Dv*

The HCP was isolated from a *D. vulgaris* clone over-producing the protein from recombinant plasmid pJS 104 [3, 11]. Crystals were grown at 277 K either in hanging drops or under paraffin oil [12]. The precipitant solution containing 0.1 M MES at pH 5.9, 0.2 M magnesium acetate and 25–30% PEG 8000 was mixed with an equal volume (3–5  $\mu\text{L}$ ) of a 12 mg/mL solution of the protein in 5 mM Tris-HCl at pH 8.0. For hanging drop conditions, a reservoir solution of equal volumes (200  $\mu\text{L}$ ) of precipitant and water was used. Initially a brown precipitate formed within the drop, from which straw-coloured crystals appeared after 4–5 days. The protein as-isolated is in the +5 oxidation state, as determined by EPR spectroscopy ([5] and references therein).

### X-ray data collection

#### The *Dd* protein: data using a wavelength of 1.722 Å

X-ray data were collected from a single cryo-cooled crystal at 100 K on beamline BM14 at the ESRF synchrotron radiation source. The wavelength selected, 1.722 Å, was just above the iron absorption K-edge. The detector (a Mar 131 mm CCD) was positioned at the minimum distance possible for the experimental set-up, 76 mm, limiting the possible resolution to 2.5 Å. The sample was previously cryo-protected by transfer (for the shortest time possible) to a solution obtained by adding 15% of glycerol to the mother liquor. Data were processed using DENZO [13] and the indexed intensities were merged and converted to structure factors using the programs ROTAPREP, SCALA and TRUNCATE in the CCP4 program suite [14]. Details of data collection are given in Table 1.

The asymmetric unit (unit cell for space group *P1*) accommodates two molecules of molecular weight 60 kDa, corresponding to a  $V_m$  of 2.03 Å<sup>3</sup> Da<sup>-1</sup> [15] and a solvent content of some 39%.

#### The *Dd* protein: data using a wavelength of 0.933 Å

Data were collected from a single cryo-cooled crystal at 100 K on the ESRF beamline ID14-2 as indicated in Table 1. Data images were treated as for the data collected with a wavelength of 1.722 Å. Radiation damage effects were assessed using the individual frame *B*-factors referred to the first image and comparing images taken

from identical  $\phi$  rotation ranges at the start and end of the data collection; there appeared to be no significant radiation damage.

#### The *Dv* protein: data using a wavelength of 0.87 Å

Data for an oxidized crystal of the *Dv* protein were collected on station 9.6 using the SRS radiation source at CLRC Daresbury Laboratory, Warrington, UK, as shown in Table 1. The data were processed using the program MOSFLM [16] and further analysis was carried out using programs from the CCP4 suite [14]. The asymmetric unit accommodates one molecule of molecular weight 60 kDa, corresponding to a  $V_m$  of 2.61 Å<sup>3</sup> Da<sup>-1</sup> [15] and a solvent content of around 53%.

Structure determination and refinement of the HCP protein from *Dd* using the data collected at a wavelength of 1.722 Å

Preliminary phases were obtained by the molecular replacement method using the program AMORE [17, 18] with the HCP model from *Dv* at 1.6 Å resolution ([6]; PDB code 1E2U) as a search probe. Hybrid and cubane Fe-S cluster atoms and solvent molecules were removed from the model prior to the molecular replacement search. The two HCPs share 64% sequence identity and two clear solutions, corresponding to the two monomers in the asymmetric unit, were identified in the rotation function (correlation coefficients of 29.9 and 29.6; next highest peak 7.1). The first molecule (A) was then fixed as the origin (as the space group is *P1*, the most convenient origin may be chosen) for the translation function search, resulting in an *R*-factor of 40.9% after a rigid body refinement. These preliminary phases were then used to calculate an anomalous difference Fourier synthesis; the anomalous signal of iron at a wavelength of 1.722 Å is  $f'' = 3.86$  electrons. This synthesis showed the presence of eight iron atoms per molecule, four each in two different clusters, at RMS levels between 19.1 and 12.3 RMS above the noise level;<sup>1</sup> the next highest peak at a level of 4.7 RMS corresponded to the *Sy* of Cys427 in monomer A.

Solvent flattening was performed using the density modification program DM [19] and a first rebuilding step was undertaken using

<sup>1</sup>The list of peaks and peak heights is included in Table S1 of the Supplementary material

**Table 2** Refinement statistics for *Dd* and *Dv* at 1.25 Å

	<i>Dd</i>	<i>Dv</i>
Amino acids	2×553	553
Protein atoms	4133 A; 4137 B	4267
Solvent atoms	1540	1015
Other atoms	2×18 + 1 acetate	19
Resolution limits (Å)	28.63–1.25	19.92–1.25
Working set <i>R</i> (observations)	0.130/223,388	0.157/155,271
Test set <i>R</i> (observations)	0.145/12,427	0.174/8,216
Highest resolution shell		
<i>R</i>	0.154/15,152	0.284/10,111
Free <i>R</i>	0.179/780	0.285/548
Cruickshank's DPI [40]	0.038	0.041
Average $B_{\text{iso}}$ (Å <sup>2</sup> )		
All atoms	9.8	16.4
Protein atoms	7.8 A; 8.0 B	13.2
Main chain	7.0 A; 7.1 B	12.2
Side chain	8.7 A; 8.9 B	14.2
Solvent	19.8	30.1
Residue not found	G544 A and B	–
Residues in alternative conformations	A: K16, V21, M90, S101, K165, N168, M174, G282, S345, E364, N436 B: V21, M90, K165, M174, E296, E340, I483	E25, E26, I35, K93, E142, I152, T173, E174, V314, E319
Residues with incomplete side chain density	A: Q20, E167, K281, K380, K386, E467, K503, K521, E525, K540 B: R61, K200, K313, K380, K386, K404, K418, N436, E467, K503, K540	K254, K280, K318, K398, K411, K553
Distance deviations <sup>a</sup>		
Bond distances (Å)	0.010	0.012
Bond angles (°)	1.564	1.462
Planar groups (Å)	0.006	0.006
Chiral volume deviation (Å <sup>3</sup> )	0.108	0.105

<sup>a</sup>RMS deviations from standard values

the program O [20]. Wherever possible, the *Dd* sequence was taken into account and a large part of the structure could be fitted into the density, but some side chains with poor density were omitted. Refinement was carried out using the program CNS [21] with the maximum likelihood target function and a bulk solvent correction. An initial rigid-body refinement to 3 Å resolution using four different rigid bodies (domain 1 was divided in two, each of the three  $\alpha$ -helix bundles being allowed to move independently; domain 2 and domain 3 were considered to be independent) resulted in a reduction of the initial *R* and  $R_{\text{free}}$  (*R*: 26.6% to 24.4%;  $R_{\text{free}}$ : 25.8% to 24.5%); as previously mentioned, cluster atoms were excluded at this stage. Rigid body refinement was followed by a simulated annealing step using torsion angle dynamics and energy minimization to reduce model errors and a grouped *B*-factor refinement step. Several cycles of cautious rebuilding of protein atoms and restrained positional and grouped *B*-factor refinement stages were subsequently performed. Grouped *B*-factor refinement was used for the main-chain and side-chain atoms of each residue, since the data resolution was not considered to be sufficiently high to allow sensible individual atomic *B*-factor refinement. The iron and sulfur cluster atoms were then added as they became clear in SigmaA-weighted [22]  $|F_o| - |F_c|$  electron density difference maps; the iron positions corresponded to those given by the anomalous difference Fourier synthesis computed before the start of refinement.

In both monomers the Cys399 residues were refined as thiocysteine and the S-S bond lengths were allowed to refine with a very low weight given to the geometrical restraints. Cluster Fe atoms were considered to be bound to the protein and to neighbouring cluster atoms, but all distances were allowed to refine almost freely. Although the Fe and S atoms in the hybrid cluster were well defined for both molecules, the  $\mu$ -bridging oxygen atoms were not easy to locate unequivocally at this resolution. Some 200 water molecules were also located based on SigmaA-weighted  $|F_o| - |F_c|$  electron density peaks higher than 3 RMS and at minimum and maximum

distances of 2.0 Å and 3.2 Å from a suitable hydrogen bonding partner. All water molecules were also present in SigmaA-weighted  $2|F_o| - |F_c|$  electron density maps.

The final model consisted of 543 of the total 544 amino acid residues in the sequence for each of the two monomers in the asymmetric unit, all the Fe and S atoms of the cubane and hybrid clusters and the water molecules. A number of surface residue side-chains had no visible electron density and were therefore omitted from the final model, as shown in Table 2. Arg61 in monomer B showed two different conformations and two *cis*-peptides were identified in each molecule: Asn307-Cys308 and Gly508-Pro509. The final  $R_{\text{factor}}$  and  $R_{\text{free}}$  were 19.3% and 25.9%, respectively.

This structure determination provided an independent confirmation of the overall molecular organization of the HCP proteins and, in particular, of the configuration of the iron and sulfur atoms in the hybrid cluster.

#### Refinement of the HCP proteins from *Dd* and *Dv* at 1.25 Å

For both HCP proteins, refinement was performed using the maximum likelihood functions implemented in REFMAC [23], starting with the model determined as described above for *Dd* and that elucidated at 1.6 Å for *Dv* [6]. Initially, all the heteroatoms in the two clusters were omitted in order to minimize any model bias and temperature factors for the starting models were set to the appropriate Wilson plot values. Rounds of conjugate gradient sparse matrix refinement with bulk solvent modelling according to the Babinet principle [24] were alternated with model building using the O program [20] in combination with SigmaA-weighted  $2|F_o| - |F_c|$  and  $|F_o| - |F_c|$  electron density maps.

As far as possible, residues were assigned according to the sequence, even when the side chain density was discontinuous or, as is the case of several surface lysine residues, incomplete at the

**Table 3** Quality of structure for *Dd* and *Dv* at 1.25 Å

	<i>Dd</i>	<i>Dv</i>
Overall <i>G</i> factor <sup>a</sup>	0.24	0.23
Ramachandran analysis % (no.) <sup>a</sup>		
Favourable	94.1 (892)	93.5 (447)
Additional	5.2 (49)	6.3 (30)
Generous	0.3 (3)	0.2 (1)
Disallowed	0.4 (4)	0.0
No. of glycine residues	2 × 49	50
No. of proline residues	2 × 18	23

<sup>a</sup>*G* factor and Ramachandran analysis were determined by PROCHECK [25]

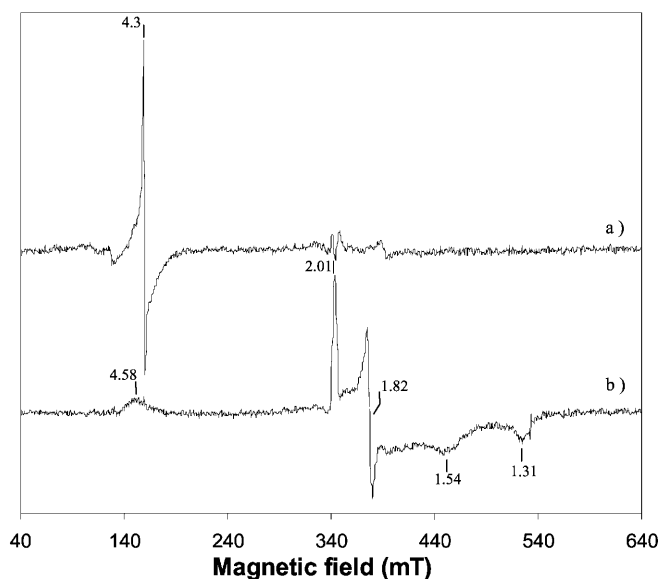


**Fig. 1** EPR spectra of the HCP purified anaerobically from *Dd*, as prepared (a) and after reduction with sodium dithionite (b). Microwave frequency: 9.64 GHz; modulation amplitude: 0.9 mT; temperature: 10 K

amino terminus. Where appropriate, side chains were included in more than one conformation. Solvent molecules were removed if their temperature coefficients exceeded 40 Å<sup>2</sup> for *Dd* and 50 Å<sup>2</sup> for *Dv*, the values at which there was poor or no electron density at the 1 RMS level in a  $2|F_o| - |F_c|$  synthesis. Additional solvent molecules were assigned on the basis of the criteria mentioned above.

All the iron atoms in both clusters and the inorganic sulfur atoms of the cubane cluster were added at an early stage. For the hybrid clusters, the bridging sulfur and oxygen atoms were only assigned after exploring the behaviour of their thermal parameters on refinement and the size of the peaks in Fourier and difference Fourier syntheses. For example, if a bridging atom was assigned as sulfur and its temperature factor refined to a value far greater than the local average of the cluster, it was reassigned as an oxygen, and vice versa. The geometries of cluster atoms were unrestrained throughout the refinement. In the final stages, all the Fe and S atoms (inorganic S and cysteine S) associated with the two clusters were allowed to refine anisotropically. For the protein, hydrogen atoms were included as “riding” atoms. Details of the final refinement statistics are given in Table 2.

#### Quality of the refined structures

The quality of both structures is high, as indicated by the PROCHECK parameters [25] listed in Table 3, and there is no



**Fig. 2** An overall view of the HCP protein from *Dd* showing the three domains. Domains 1, 2 and 3 are coloured green, blue and pink, respectively. The cubane cluster is located at the N-terminus of domain 1, close to the exterior of the molecule, whereas the hybrid cluster lies at the interface of the three domains. The hybrid cluster is accessible through both hydrophobic cavities and hydrophilic channels [6]

significant difference between the *Dv* reported herein and that previously described at 1.6 Å resolution [6]. In the *Dd* structure the two molecules in the asymmetric unit are almost identical so the C $\alpha$  atoms of molecule B superimpose on molecule A with an RMS deviation of 0.55 Å. The only major difference is that the loop at residues 335–339 in molecule B appears disordered, whereas in A it is in well-defined electron density. In the current model this region in molecule B has been built according to molecule A, with no attempt made to model alternative conformations. There is also a relatively poorly defined region involving a close inter-molecular contact between molecule A, residues Thr135, Asp136 and Asp137, and molecule B, Gln536, in a different asymmetric unit (*x*, 1–*y*, 1–*z*). In both *Dd* and *Dv* structures there are a number of residues with more than one conformation and those modelled most readily are listed in Table 2. Table 2 also lists several residues, mainly lysines, where the side chain density is very poor or non-existent at the 1 RMS level. In the *Dd* structure there are two residues in each molecule in the disallowed region of the Ramachandran plot [26], Ser263<sup>2</sup> and Asn299. In the *Dv* structure the residue equivalent to Asn299, Asn303, is close to the border between the left-handed helix (L) region of the plot and the disallowed region. However, in each case the residues lie in well-defined electron density; Ser263 is located on a bend between a  $\beta$ -strand and an  $\alpha$ -helix, whereas the asparagine residues occur on bends between  $\alpha$ -helices and  $\beta$ -strands.

Information for the three data sets and the associated structures has been deposited in the Protein Data Bank with deposition codes 1GN9, 1GNL and 1GNT for the *Dd* enzyme using X-ray wavelengths of 1.722 Å and 0.933 Å, and the *Dv* enzyme using a wavelength of 0.87 Å, respectively.

<sup>2</sup>Figure S1, showing the electron density in the vicinity of Ser263 in molecule A of *Dd*, is included in the Supplementary material. The relevant  $\phi/\psi$  torsion angles are also listed

**Table 4** Geometry (bond lengths in Å) of the cubane and hybrid cluster in the HCP proteins *Dd* and *Dv* at a resolution of 1.25 Å

Cubane cluster	<i>Dd</i> (A)	<i>Dd</i> (B)	<i>Dv</i>
Fe1-Fe2	2.73	2.73	2.74
-Fe3	2.69	2.70	2.70
-Fe4	2.77	2.76	2.78
-S1	2.30	2.31	2.32
-S2	2.29	2.28	2.26
-S3	2.32	2.33	2.33
-Cys SG	2.28 (Cys6)	2.29	2.29 (Cys3)
Fe2-Fe3	2.71	2.72	2.69
-Fe4	2.69	2.70	2.66
-S1	2.28	2.26	2.29
-S2	2.36	2.35	2.34
-S4	2.32	2.33	2.32
-Cys SG	2.26 (Cys9)	2.26	2.27 (Cys6)
Fe3-Fe4	2.73	2.74	2.71
-S1	2.33	2.34	2.33
-S3	2.32	2.32	2.33
-S4	2.27	2.27	2.27
-Cys SG	2.31 (Cys18)	2.30	2.36 (Cys15)
Fe4-S2	2.36	2.34	2.33
-S3	2.26	2.26	2.28
-S4	2.34	2.35	2.35
-Cys SG	2.30 (Cys24)	2.29	2.31 (Cys21)
Hybrid cluster	<i>Dd</i> (A)	<i>Dd</i> (B)	<i>Dv</i>
Fe5-Fe6	2.76	2.77	2.75
-Fe7	3.63	3.67	3.64
-Fe8	3.35	3.36	3.12
-S5	2.31	2.31	2.31
-S6	2.32	2.31	2.30
-Cys SG	2.32 (Cys427)	2.33	2.32 (Cys434)
-O10	–	–	1.90
-O11	2.00	1.99	1.94
Fe6-Fe7	4.94	4.86	5.12
-Fe8	3.02	3.02	3.15
-S5	2.25	2.25	2.19
-S6	2.27	2.26	2.25
-Cys SG	2.33 (Cys308)	2.33	2.31 (Cys312)
-O8	1.98	1.93	2.11
Fe7-Fe8	3.55	3.56	3.37
-Cys SG	2.45 (Cys452)	2.42	2.45 (Cys459)
-His NE2	2.13 (His240)	2.16	2.18 (His244)
-Glu OE2	2.15 (Glu264)	2.16	2.16 (Glu268)
-O9	2.13	2.14	2.17
-O10	–	–	1.86
-O11	2.06	2.08	2.10
Fe8-S6	2.42	2.44	2.42
-S7	2.54	2.54	2.56
-Glu OE2	2.04 (Glu487)	2.02	2.09 (Glu494)
-O8	2.19	2.17	2.24
-O9	1.93	1.95	1.89
-O10	–	–	2.22
S7-Cys SG	2.09 (Cys399)	2.09	2.10 (Cys406)
O8-Asn ND2	3.02 (Asn307)	3.04	2.88 (Asn311)
O9-Lys NZ	2.99 (Lys489)	2.95	2.95 (Lys496)
O10-O11	–	–	1.13

## Results and discussion

EPR characterization of anaerobically prepared *Dd* HCP

*Dd* HCP was successfully purified anaerobically, as described in Materials and Methods. SDS-PAGE showed a single band, proving the protein purity (data

not shown). EPR spectroscopy of the as-purified protein suggests that the hybrid cluster is in the two-electron reduction (+4 oxidation) state, i.e. in the EPR-silent state as shown in Fig. 1a. Upon reduction with sodium dithionite the characteristic spectra of the hybrid cluster in the three-electron reduced (+3 oxidation) state with  $g_{\max}=2.01$  was observed, together with the  $g=4.58$  feature associated with the cubane centre with system spin  $S=3/2$  (Fig. 1b). Oxidation under air to yield the one-electron reduced (+5 oxidation) state or the fully oxidized (+6) state was extremely slow, taking several hours; even after 24 hours of exposure to air, the fully oxidized +6 state could not be observed. Prolonged exposure or oxidation with potassium ferricyanide led to the appearance of the resonances characteristic of the one-electron reduced state. Reduction of the air-oxidized protein led to spectra having the features of the fully reduced enzyme. These data suggest that the structures of the HCP clusters are not affected by oxygen, at least as far as their magnetic properties, as monitored by EPR spectroscopy, are concerned. Furthermore, HCP clusters appear to be highly unreactive with oxygen, i.e. reoxidation by oxygen is extremely slow, which at least in part is probably due to the high reduction potential of the +5/+6 transition [3].

## Overall molecular architecture

The three-dimensional structures of the HCPs from *Dd* and *Dv* show a very high similarity. Thus the *Dv* structure superimposes on molecules A and B of the *Dd* structure with RMS deviations of 0.89 Å (528) and 0.84 Å (529), respectively, where the numbers in parentheses indicate the number of  $\alpha$ -carbons atoms in the fit. The fit per domain is even better than this so that, for example, domain 2 of *Dv* superimposes on the corresponding domains of *Dd* with RMS deviations of 0.48 Å (128) and 0.56 Å (129), respectively. Each structure comprises three domains, with a cubane iron-sulfur cluster located in domain 1 near the exterior surface of the molecule and the hybrid cluster deeply buried at the interface between the three domains (Fig. 2). Domain 1 is predominantly  $\alpha$ -helical, with two unusually disposed three-helix bundles almost orthogonal to each other. The four cubane cluster cysteine ligands, Cys6, Cys9, Cys18 and Cys24 (*Dd* numbering), are all conserved throughout the HCPs. Domains 2 and 3 are organized in a similar way, both consisting of a central  $\beta$ -sheet with helices on either side. The hybrid cluster ligands, His240, Glu264, Cys308, Cys399, Cys427, Cys452 and Glu487 (*Dd* numbering), are also conserved in all known HCPs.

## Iron-sulfur clusters

In each structure, the cubane cluster is a conventional  $[4\text{Fe-4S}]^{2+/1+}$  cluster, bound by four cysteine residues at the N-terminus of the molecule in a CysX<sub>2</sub>CysX<sub>8</sub>-CysX<sub>5</sub>Cys motif. As in other cubane clusters, three

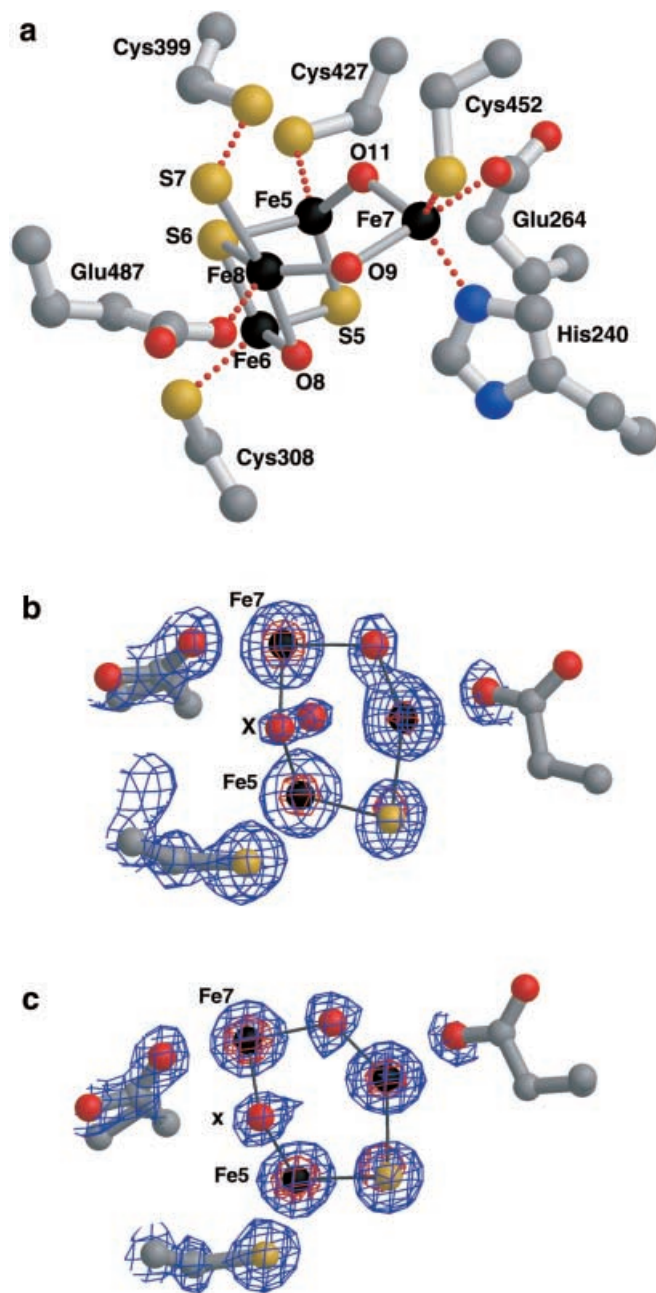


**Fig. 3a–c** The hybrid cluster in the HCP proteins. **a** A schematic view of the cluster in *Dd*; **b** electron density in a  $2|F_o| - |F_c|$  map contoured at the 2.0 (blue) and 15.0 (red) RMS levels in the vicinity of the X moiety in the *Dv* protein; **c** as per **b** for molecule A in the *Dd* protein

inorganic sulfurs coordinate each iron. The Fe–Fe, Fe–S and Fe–S (Cys) distances average 2.72, 2.31 and 2.29 Å, respectively (see Table 4). The cubane clusters have a closest approach of 11.6 Å to the hybrid clusters (Fe2–Fe8 and Fe4–Fe6, where Fe2 and Fe4 belong to the cubane clusters, and Fe6 and Fe8 to the hybrid clusters).

The hybrid clusters are coordinated by seven amino acids lying at the interfaces of the three domains. The overall structure appears to be independent of the oxidation state of the protein and/or whether the

preparations were performed aerobically or anaerobically. The Fe–Fe separations range between 2.75 Å and 5.12 Å and the hybrid cluster contains both  $\mu$ -O and  $\mu$ -S bridges between pairs of iron atoms. Figure 3a shows the main features of the hybrid clusters. They can be considered as being derived from a cube, but with an iron atom at one corner peeled back. Thus:

1. Fe5, linked to the protein by Cys427 (Cys 434 in *Dv*), and Fe6, linked by Cys308 (Cys 312 in *Dv*), together with S5 and S6, form a [2Fe–2S] moiety that constitutes a face of the cube.
2. Fe8, bound to S6 of the [2Fe–2S] moiety, lies at another corner of the cube and is linked to the protein by Glu487 (Glu494) and a persulfide moiety at Cys399 (Cys406).
3. Fe7, linked to the protein by His240 (His 244), Glu264 (Glu268) and Cys452 (Cys 459), can be considered as the fourth corner of the cube peeled away so that it lies close to the diagonal of the face formed by Fe5, S6 and Fe8 that bisects the two iron atoms.

Oxygen atoms bridge Fe6 and Fe8, and Fe7 and Fe8, and a further moiety, X, appears to bridge Fe5 and Fe7; in this case the environments of the iron atoms can be described as distorted tetrahedral for Fe5 and Fe6, distorted trigonal bipyramidal for Fe7 and distorted octahedral for Fe8. In the absence of X the coordination geometries of Fe7 and Fe 5 are incomplete and that of Fe8 can be described as trigonal bipyramidal.

The major difference between the *Dd* and *Dv* structures lies in the moiety X, bound between Fe5 and Fe7. Resonance Raman (RR) spectroscopy [27] on the aerobically prepared *Dd* and *Dv* proteins in the +5 oxidation state shows a band around  $800\text{ cm}^{-1}$ . This has been interpreted as showing the presence of a mono-bridged oxygen centre formed by an exchangeable solvent molecule, with an Fe–O–Fe angle in the  $150\text{--}180^\circ$  range. In the initial *Dv* structure at a resolution of 1.7 Å [5], X was modelled as a single oxygen atom. Repetition of this structure determination with crystals from a new batch of aerobically isolated protein led to a structure at a resolution of 1.6 Å [6]; with these data, careful refinement indicated that the oxygen atom was probably disordered between two positions. In the current *Dv* structure at a resolution of 1.25 Å, with the protein prepared aerobically, an elongated electron density peak is also observed between Fe5 and Fe7 (Fig. 3b). This density is best fitted with two oxygen atoms, O10 and O11, separated by some 1.1 Å, and with occupancies of only 50%.

In the case of the *Dd* structure prepared anaerobically in the +4 oxidation state, the best interpretation of the electron density (Fig. 3c) comprises a single oxygen atom corresponding to the O11 position in *Dv*. However, the density at O11 is not spherical, but slightly elongated towards the position that would be occupied by O10. Indeed, a difference  $|F_o| - |F_c|$  electron





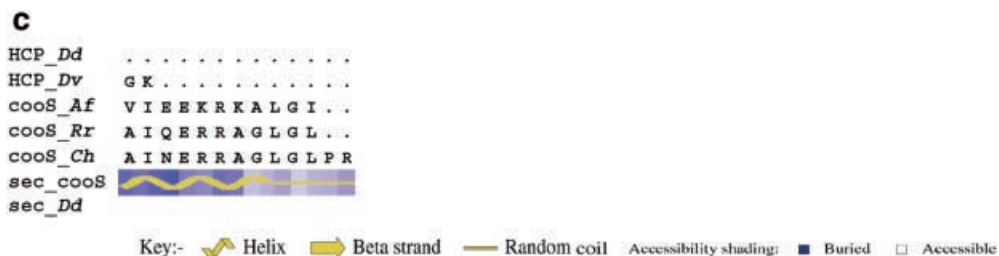


**Fig. 4** Structurally based amino acid sequence alignment of HCPs from *D. desulfuricans* ATCC 27774 (HCP\_Dd) with *D. vulgaris* Hildenborough HCP (HCP\_Dv), and the carbon monoxide dehydrogenase catalytic subunit (CODH-cooS) from *C. hydrogeniformans* (cooS\_Ch). Amino acid sequence alignments are also shown for the CODH-cooS from *Archaeoglobus fulgidus* (cooS\_Af) and *Rhodospirillum rubrum* (cooS\_Rr). (% identity to HCP\_Dd, NCBI-GI), HCP\_Dd (400847), HCP\_Dv (64%, 3915811), cooS\_Af (15%, 11499434), cooS\_Rr (17%, 399279) and cooS\_Ch (16%, 11095246). The secondary structure and the accessibility of the amino acid residues for the HCP Dd structure and the CODH-cooS from *C. hydrogeniformans*, given by PROCHECK [25], are shown below the alignment. The ligands for the normal [4Fe-4S] and the hybrid cluster ligands from HCP Dd and Dv are highlighted in black. Grey boxes represent completely conserved amino acids. The structural alignment and amino acid sequence alignments were achieved using the O [20] and ClustalW [38] programs, respectively. Sequence analysis and editing was performed using GeneDoc [39]

The hybrid cluster itself has an open configuration and is readily accessible by both hydrophobic cavities and hydrophilic channels [6]. The position of the X moiety, in between Fe5 and Fe7, represents an obvious site of substrate binding and Fe8 may also be involved, but the nature of the substrate and the reaction mechanism that it undergoes both remain to be clarified. Entry of a linear molecule such as nitrous oxide can well be envisaged with the oxygen binding to Fe8. This could be followed by dissociation of the substrate into nitrogen, which leaves through the hydrophobic cavity, and the oxygen atom remaining bound, at least temporarily, in the position of X. However, whether X results from N<sub>2</sub>O remains an open question and similar arguments could apply to a number of alternative small-molecule substrates.

#### Comparison with similar iron-sulfur clusters

The Dd/Dv hybrid cluster has many features in common with the nickel-iron-sulfur cluster found recently in the structure of carbon monoxide dehydrogenase from *Carboxydotherrmus hydrogeniformans* [28] and the “open” cluster found in the structure of the hydrogenase also isolated aerobically from Dd [29]. The asymmetric [Ni-4Fe-5S] cluster found in *C. hydrogeniformans* is, like the hybrid cluster in HCP, deeply buried in the protein at the subunit interface. Its [3Fe-3S] moiety comprising Fe2, Fe3 and Fe4 (equivalent to Fe5, Fe6 and Fe8 in the HCP proteins) and three S atoms forms three quarters of a cubane [4Fe-4S] cluster. The Ni atom is integrated into this arrangement, forming the fourth corner of the cubane-like cluster. It is coordinated by four S atoms.

An isolated iron atom, Fe1, equivalent to Fe7 in the HCP proteins, is bridged to Fe4 and the Ni by sulfur atoms at considerably longer distances than those of the other three Fe atoms in the cluster.

The open cluster in the hydrogenase also contains a [2Fe-2S] moiety (involving Fe3, Fe4, S3 and S4 in the hydrogenase numbering) and a third iron atom, Fe1 (equivalent to Fe8 in HCP), forming part of a [3Fe-3S] cluster. It differs in the nature of the bridging atoms and the amino acid residues that bind to these two iron atoms. Thus, one of the bridging oxygen atoms (equivalent to O8 in the HCP proteins) is a sulfur (S2) in the hydrogenase whereas at Fe8, E487 is a cysteine (C17) and there is no persulfide group, and at Fe7, C452 is replaced by an oxidized cysteine (C20); the X position in the hydrogenase is assigned as an oxygen atom (O24). In the hydrogenase, the open cluster is in close proximity, around 10 Å, to the [NiFe] active centre and might have a bearing on the activation process of the enzyme, rather than just being the final component of an electron transport chain. However, it is also possible that it could be an artefact, resulting from prolonged exposure to oxygen in the aerobic purification and crystallization processes. Whatever the case for the hydrogenase, the open hybrid clusters in HCPs appear to be invariant to the presence or absence of oxygen in the preparation and crystallization procedures, although an intriguing question is whether they were originally formed by oxidation of a simple cubane cluster. Further, whereas the cluster in the hydrogenase is part of an electron transport chain leading to the [NiFe] active centre, it is likely that in HCPs the hybrid clusters will be the active centres.

#### Comparison with carbon monoxide dehydrogenases

Since strains of both Dd and Dv have been reported to contain carbon monoxide dehydrogenase [CODH] activity [30], it seemed reasonable to look for eventual sequence analogies between HCPs and these enzymes. A search of the amino acid sequences databases gave significant hits with the catalytic subunits [CODH-cooS] of some of the CODH. Three representative examples of these enzymes, *Archaeoglobus fulgidus* [31], *Rhodospirillum rubrum* [32] and *C. hydrogeniformans* [33], are compared in Fig. 4 with the Dd [34] and Dv [11] HCPs. This figure shows a structurally based sequence alignment between the HCP and the CODH enzyme from *C. hydrogeniformans*. The structural alignment high-

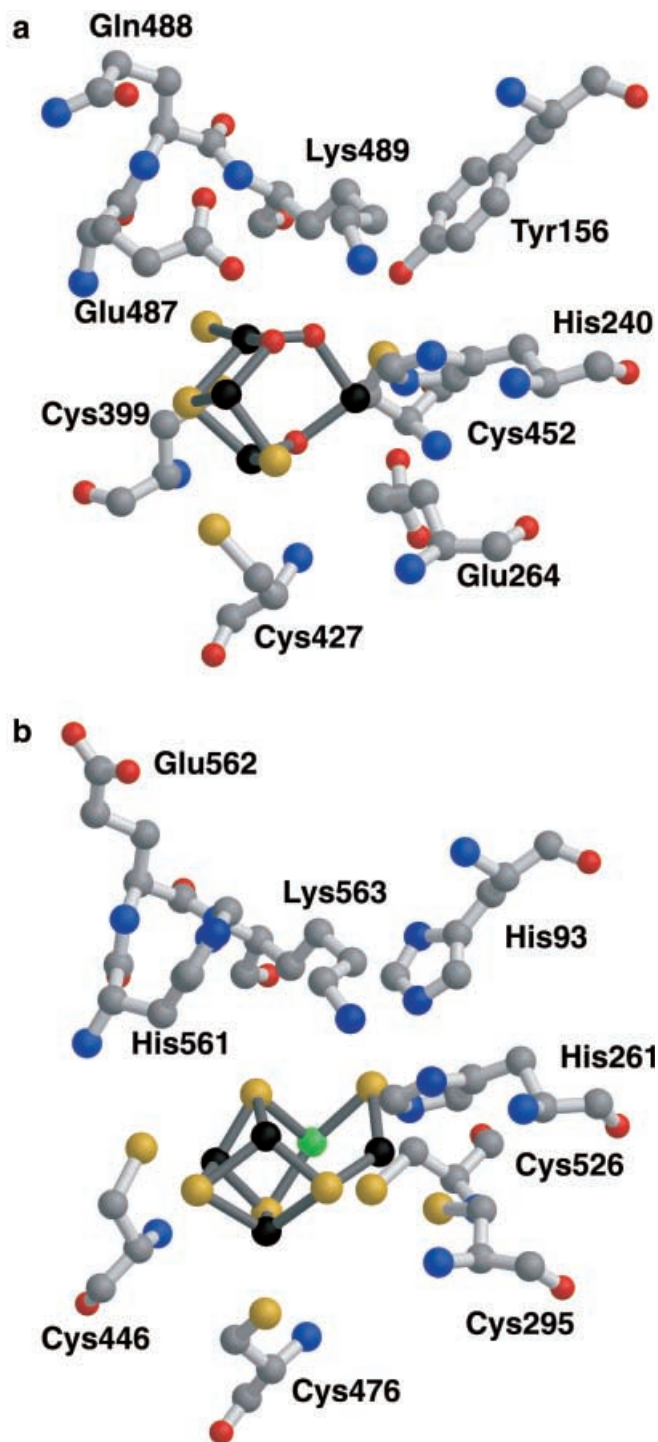


**Fig. 5** The hybrid clusters of the HCP *Dd* (a) and the CODH-cooS from *C. hydrogenoformans* (b) after structural alignment

lights the close similarity of the tertiary and secondary structural elements between *Dd/Dv* and *C. hydrogenoformans* (Fig. 5), although one of the two orthogonal three-helix bundles in domain 1 of the HCP is absent in *C. hydrogenoformans* CODH. In the vicinity of the hybrid cluster, all the cysteine (Cys308, 399, 427 and 452) and histidine (H240) cluster-binding residues are

conserved; Cys308 is not shown in the figure for reasons of clarity. Glu264 is replaced by a cysteine, which completes the six *C. hydrogenoformans* ligands for the Ni cluster-binding environment. Glu487, the final *Dd/Dv* hybrid cluster ligand, is replaced by a histidine residue that does not bind directly to the *C. hydrogenoformans* Ni cluster but is located some 5 Å distant from the Ni atom. Interestingly, Tyr156 in *Dd/Dv* is replaced by His93 in *C. hydrogenoformans*, a residue that is thought to be essential in defining the Ni active site environment [28]. This could also point towards a role for the tyrosine to orientate a (different) substrate binding in the *Dd/Dv* active site. Many of the residues contributing to the strong hydrophobicity of one of the cavities pointing towards Fe8 [6] are conserved. This cavity is formed mostly between the  $\alpha$ -helices of residues 452–468 and 487–499, as well as several residues from a back wall of a  $\beta$ -sheet and one from a long  $\alpha$ -helix crossing the entire molecule. In addition, this cavity leads directly from the surface of the protein along the  $\alpha$ -helices to Lys489 (Fig. 5), a residue that is conserved between all five enzymes and located within 3.0 Å of the oxygen atom bridging Fe7 and Fe8 in the HCP. This Lys residue is predicted to have a crucial role in the CODH enzyme mechanism and may indicate a hydrophobic pathway for substrate or product with a common key role for Lys489 between the carbon monoxide dehydrogenases and the HCP reaction mechanisms.

All the enzymes in the sequence alignment possess cysteine residues, albeit with different sequence spacings, at their N-termini capable of binding a canonical [4Fe-4S] cluster. Additionally, the sequence alignment shows that *Archaeoglobus fulgidus* also possesses all the ligands characteristic for binding a hybrid cluster. For *Rhodospirillum rubrum*, as in *C. hydrogenoformans*, Glu264 (*Dd* numbering), a potential ligand to Fe7 of the cluster, is replaced by a cysteine residue. There does, however, appear to be a distinction in several of the crucial cluster binding and environment ligands highlighted by the alignment where *Dd*, *Dv* and *Archaeoglobus fulgidus* share conserved residues and *Rhodospirillum rubrum* and *C. hydrogenoformans* are different, namely Tyr156 (His), Glu264 (Cys), Glu487 (Ser/His) and Gln488 (Glu), as shown in Fig. 4. This might suggest that *Archaeoglobus fulgidus* is evolutionary closer to HCP than the CODH proteins and, given the potentially different cluster environment, may be able to catalyze a reaction similar to both proteins but not identical to either.

This comparison suggests that HCPs may catalyze a reaction similar to that of the CODH-cooS, namely the activation of small molecules. However, so far, any attempts to find such activity have failed.

## Conclusions

The hybrid cluster proteins from *Dd* and *Dv* both contain an unusual [4Fe-2S-2O] cluster that contains both  $\mu$ -sulfur and  $\mu$ -oxygen bridges; this nomenclature does

not include X or the S of the persulfide moiety. The nature of this cluster appears to be independent of whether the proteins are isolated aerobically or anaerobically and also the oxidation state of the cluster. In the case of the *Dd* protein, all reasonable attempts were made to minimize and monitor any effects of radiation damage. However, changes to the redox state of the clusters due to X-ray exposure should always be considered in any structural interpretation. The precise function(s) of the HCPs remains to be defined, but it is likely that the hybrid cluster is the active site and the possibility of a sulfur transferase involving the persulfide moiety cannot be discounted. Sequence comparisons with the catalytic domains of the carbon monoxide dehydrogenases from *A. fulgidus* and *R. rubrum*, together with the known structure of that from *C. hydrogeniformans*, strongly suggest that these enzymes may also contain unusual Fe-S clusters.

**Acknowledgements** We would like to thank the Biotechnology and Biological Research Council (UK) for support (S.J.C.) and to our colleagues at the CLRC Daresbury Laboratory (UK) and the ESRF, Grenoble (France) for the provision of synchrotron radiation facilities. The support of FCT-Portugal, project 36558/99, is acknowledged (M.T.), as is PRAXIS XXI, grant BD/19879/99 (C.V.R.). The authors would like to thank the University of Georgia, Athens, USA, for access to the fermentation plant where the *Dd* bacteria were grown. The NIH (USA) is acknowledged for a grant (GM 5600) to J.L.G. and M.Y.L. and IBET (Portugal) for a grant to M.Y.L. Figures 2, 3, 5 and S1 were drawn with the help of MolScript [35], BobScript [36] and Raster3D [37].

## References

- Hagen WR, Pierik AJ, Veeger C (1989) *J Chem Soc Faraday Trans I* 85:4083–4090
- Moura I, Tavares P, Moura JJ, Ravi N, Huynh BH, Liu MY, LeGall J (1992) *J Biol Chem* 267:4489–4496
- Pierik AJ, Wolbert RB, Mutsaers PH, Hagen WR, Veeger C (1992) *Eur J Biochem* 206:697–704
- Pierik AJ, Hagen WR, Dunham WR, Sands RH (1992) *Eur J Biochem* 206:705–719
- Arendsen AF, Hadden J, Card G, McAlpine AS, Bailey S, Zaitsev V, Duke EHM, Lindley PF, Kröckel M, Trautwein AX, Feiters MC, Charnock JM, Garner CD, Marritt SJ, Thomson AJ, Kooter IM, Johnson MK, van den Berg WAM, van Dongen WMAM, Hagen WR (1998) *J Biol Inorg Chem* 3:81–95
- Cooper SJ, Garner CD, Hagen WR, Lindley PF, Bailey S (2000) *Biochemistry* 39:15044–15054
- Tavares P, Pereira AS, Krebs C, Ravi N, Moura JJ, Moura I, Huynh BH (1998) *Biochemistry* 37:2830–2842
- van den Berg WAM, Hagen WR, van Dongen WAM (2000) *Eur J Biochem* 267:666–676
- Liu MC, Peck HD Jr (1981) *J Biol Chem* 256:13159–13164
- LeGall J, Liu MY, Gomes CM, Braga V, Pacheco I, Regalla M, Xavier AV, Teixeira M (1998) *FEBS Lett* 429:295–298
- Stokkermans JPWG, Pierik AJ, Wolbert RBG, Hagen WR, van Dongen WMAM, Veeger C (1992) *Eur J Biochem* 208:435–442
- Arendsen A, Bulsink Y, Hagen W, Hadden J, Card G, McAlpine AS, Bailey S, Zaitsev V, Lindley P (1996) *Acta Crystallogr Sect D* 52:1211–1213
- Otwinowski Z, Minor W (1997) *Methods Enzymol* 276:307–326
- Collaborative Computational Project number 4 (1994) *Acta Crystallogr Sect D* 50:760–763
- Matthews BW (1968) *J Mol Biol* 33:491–497
- Leslie AGW (1991) In: Moras D, Podjarny AD, Thierry JC (eds) *Crystallographic computing V*. Oxford University Press, Oxford, pp 27–38
- Castellano EE, Oliva G, Navaza J (1992) *J Appl Crystallogr* 25:281–284
- Navaza J (1993) *Acta Crystallogr Sect D* 49:588–591
- Cowtan KD, Main P (1996) *Acta Crystallogr Sect D* 52:43–48
- Jones TA, Zou JY, Cowan SW, Kjeldgaard M (1991) *Acta Crystallogr Sect A* 47:110–119
- Brünger AT, Adams PD, Clore GM, DeLano WL, Gros P, Grosse-Kunstleve RW, Jiang JS, Kuszewski J, Nilges M, Pannu NS, Read RJ, Rice LM, Siminson T, Warren GL (1998) *Acta Crystallogr Sect D* 54:905–921
- Read RJ (1986) *Acta Crystallogr Sect A* 42:140–149
- Murshudov GN, Vagin AA, Dodson EJ (1997) *Acta Crystallogr Sect D* 53:240–255
- Tronrud D (1996). In: Dodson E, Moore M, Ralph A, Bailey S (eds) *Macromolecular refinement. Proceedings of CCP4 study weekend*. Daresbury Laboratory, Warrington, UK, pp 1–10
- Laskowski RA, MacArthur MW, Moss DS, Thornton JM (1993) *J Appl Crystallogr* 26:283–291
- Ramakrishnan C, Ramachandran GN (1965) *Biophys J* 5:909–933
- de Vocht ML, de Kooter IM, Bulsink YBM, Hagen WR, Johnson MK (1996) *J Am Chem Soc* 118:2766–2767
- Dobbek H, Svetlichnyi V, Gremer L, Huber R, Meyer O (2001) *Science* 293:1281–1285
- Matias PM, Soares CM, Saraiva LM, Coelho R, Morais J, LeGall J, Carrondo MA (2001) *J Biol Inorg Chem* 6:63–81
- Meyer O, Rohde M (1984) In: Crawford RL, Hanson RS (eds) *Microbial growth on C1 compounds; proceedings of the 4th international symposium*. American Society for Microbiology, Washington, pp 26–33
- Klenk H-P, Clayton RA, Tomb J-F, White O, Nelson KE, Ketchum KA, Dodson RJ, Gwinn M, Hickey EK, Peterson JD, Richardson DL, Kerlavage AR, Graham DE, Kyrpides NC, Fleischmann RD, Quackenbush J, Lee NH, Sutton GG, Gill S, Kirkness EF, Dougherty BA, McKenney K, Adams MD, Loftus B, Peterson S, Reich CI, McNeil LK, Badger JH, Glodek A, Zhou L, Overbeek R, Gocayne JD, Weidman JF, McDonald L, Utterback T, Cotton MD, Spriggs T, Artiach P, Kaine BP, Sykes SM, Sadow PW, D'Andrea KP, Bowman C, Fujii C, Garland SA, Mason TM, Olsen GJ, Fraser CM, Smith HO, Woese CR, Venter JC (1997) *Nature* 390:364–370
- Fox JD, Kerby RL, Roberts GP, Ludden PW (1996) *J Bacteriol* 178:1515–1524
- Gonzalez JM, Robb FT (2000) *FEMS Microbiol Lett* 191:243
- Stokkermans JPWG, van den Berg WAM, van Dongen WMAM, Veeger C (1992) *Biochim Biophys Acta* 1132:83–87
- Kraulis PJ (1999) *J Appl Crystallogr* 24:946–950
- Esnouf RM (1999) *Acta Crystallogr Sect D* 55:938–940
- Merritt EA, Bacon DJ (1997) *Methods Enzymol* 277:505–524
- Thompson JD, Higgins DG, Gibson TJ (1994) *Nucleic Acids Res* 22:4673–4680
- Nicholas KB, Nicholas HB Jr, Deefield DW (1997) *EMBNEW.NEWS* 4:14 (<http://www.psc.edu/biomed/genedoc/gdfeeddb.htm>)
- Cruickshank DWJ (1996) In: Dodson E, Moore M, Ralph A, Bailey S (eds) *Macromolecular refinement. Proceedings of the CCP4 study weekend, January 1996*. CLRC Daresbury Laboratory, Warrington, UK, pp 11–22